

Variable Stiffness Suspension System

Olugbenga Moses Anubi

Contents

1	Introduction	2
2	Variable Stiffness Suspension System: Passive Case	2
2.1	Experiment	3
2.2	Simulation	4
3	Variable Stiffness Suspension System: Active Case	5
3.1	Control Design	8
3.2	Simulation	8
4	Variable Stiffness Suspension System: Semi-active Case	10
4.1	Control Design	11
4.2	Simulation	11
5	Roll Stabilization Using Variable Stiffness Suspension System	13
5.1	Mechanism Description	14
5.2	Modeling	15
5.3	Parameter Estimation	16
5.4	Control Design	16
5.5	Simulation	18
5.5.1	Fish hook Maneuver	18
5.5.2	Double Lane Change Maneuver	19
6	Biography Sketch	20

1 Introduction

Improvements over passive suspension designs is an active area of research. Past approaches utilize one of three techniques; adaptive, semi-active, or fully active suspension. An adaptive suspension utilizes a passive spring and an adjustable damper with slow response to improve the control of ride comfort and road holding. A semi-active suspension is similar, except that the adjustable damper has a faster response and the damping force is controlled in real-time. A fully active suspension replaces the damper with a hydraulic actuator, or other types of actuators like electromagnetic actuators, which can achieve optimum vehicle control, but at the cost of design complexity. Recently, research in semi-active suspensions has continued to advance with respect to capabilities, narrowing the gap between semi-active and fully active suspension systems. However, most semi-active design concepts are focused on only varying the damping coefficient of the shock absorber while keeping the stiffness constant. Today, semi-active suspensions (e.g using Magneto-Rheological (MR), Electro-Rheological (ER) etc) are widely used in the automobile industry due to their small weight and volume, as well as low energy consumption compared to purely active suspension systems.

However, most semi-active suspension systems are designed to only vary the damping coefficient of the shock absorber while keeping the stiffness constant. Meanwhile, in suspension optimization, both the damping coefficient and the spring rate of the suspension elements are usually used as optimization arguments. Therefore, a semi-active suspension system that varies both the stiffness and damping of the suspension element could provide more flexibility in balancing competing design objectives. Suspension designs that exhibit variable stiffness phenomenon are few in literature considering the vast amount of researches that has been done on semi-active suspension designs. This excerpt gives a brief summary of the research I did at the Center for Intelligent Machines and Robotics (CIMAR) within January, 2010 and March, 2013 concerning the design, analysis, experimentation and application of a high efficient, low-power variable stiffness suspension system.

2 Variable Stiffness Suspension System: Passive Case

This work considers the design, analyses, and experimentation of a new variable stiffness suspension system. The design is based on the concept of a variable stiffness mechanism. The system is analyzed using an \mathcal{L}_2 -gain analysis based on the concept of energy dissipation. The analyses, simulation, experimental results, show that the variable stiffness suspension achieves better performance than the constant stiffness counterpart. The performance criteria used are; ride comfort, characterized by the car body acceleration, suspension deflection, and road holding, characterized by tire deflection. The variable stiffness mechanism concept is shown in Fig 1a. The idea is to vary the overall stiffness of the system by letting d vary passively under the influence of a horizontal spring-damper system as shown in Fig. 1b. Fig. 1c shows a schematic of the suspension system, where

u denotes the horizontal force¹ which is generated by a passive spring-damper system.

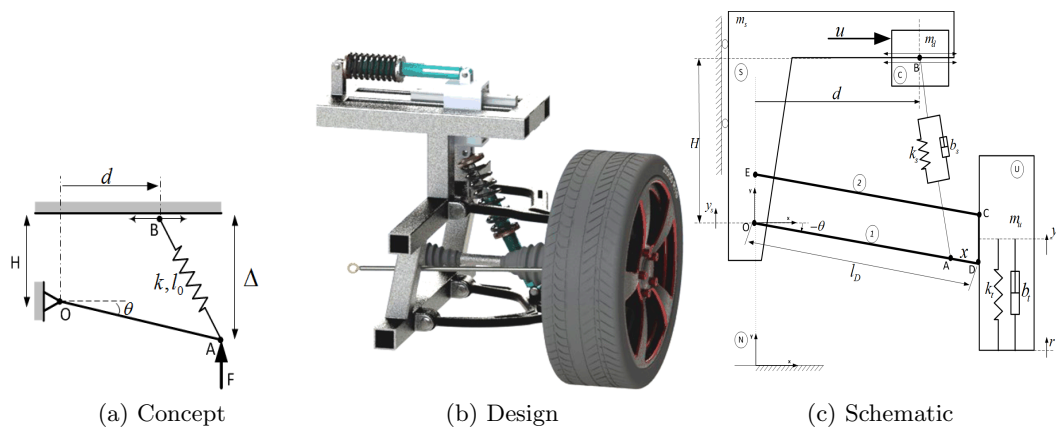


Figure 1: Variable Stiffness Suspension System

2.1 Experiment

The experimental setup is shown in Fig. 2. It is a quarter car test rig scaled down to a ratio of 1:10 compared to an average passenger car. The quarter car body is allowed to translate up-and-down along a rigid frame. This was made possible through the use of two pairs of linear motion ball-bearing carriages, with each pair on separate parallel guide rails. The guide rails are fixed to the rigid frame and the carriages are attached to the quarter car frame. The quarter car frame is made of 80/20 aluminium framing and then loaded with a solid steel cylinder weighing approximately 80lbs. The horizontal and vertical struts are the 2011 Honda PCX scooter front suspensions. The road generator is a simple slider-crank mechanism actuated by Smartmotor[®] SM3440D geared down to a ratio of 49:1 using CMI[®] gear head P/N 34EP049 . Three accelerometers are attached, one each to the quarter car frame, the wheel hub, and the road generator. Data acquisition was done using the MATLAB data acquisition toolbox via NI USB-6251. Experiments were performed for the passive case, where the horizontal strut is just a passive spring-damper system, and also for the fixed stiffness case, where the top of the vertical strut is locked in a fixed position. This position is the equilibrium position of the unexcited passive case.

Two tests were carried out; sinusoidal, and drop test. For the sinusoidal test, the road generator is actuated by a constant torque from the DC motor. As a result, the quarter car frame moves up and down in a sinusoidal fashion. For the drop test, the suspension system was dropped to the ground² from a fixed height (6 inches from the

¹The horizontal force can also be generated by either a semi-active or an active device. The corresponding cases are considered later.

²Here the ground is non accelerating as against the sinusoidal test where the ground simulates the



Figure 2: Quarter Car Experimental Setup

equilibrium position and the wheel was not in contact with the ground). The resulting quarter car body acceleration and tire deflection accelerations were recorded. This test examines the response of the system to initial conditions. Figure 3a and Figure 3b shows the car body acceleration responses and tire deflection acceleration responses for the fixed and variable stiffness cases.

Table 1 shows the approximate gains for the sinusoidal and the rms values of the drop test. The approximate gains of the sinusoidal test given in the table are the mean values of the multiple experiments.

2.2 Simulation

In order to study the behavior of the quarter car system at full scale as well as responses like suspension deflection, which were difficult to measure experimentally, and excitation scenarios that are difficult to implement experimentally, realistic simulations were carried out using MATLAB Simmechanic, Second Generation. First, the system was modeled in Solidworks. Next, the Simmechanic model was developed. The mass, vertical strut and tire damping and stiffness used are the ones given in the “Renault Mégane Coupé” road signal.

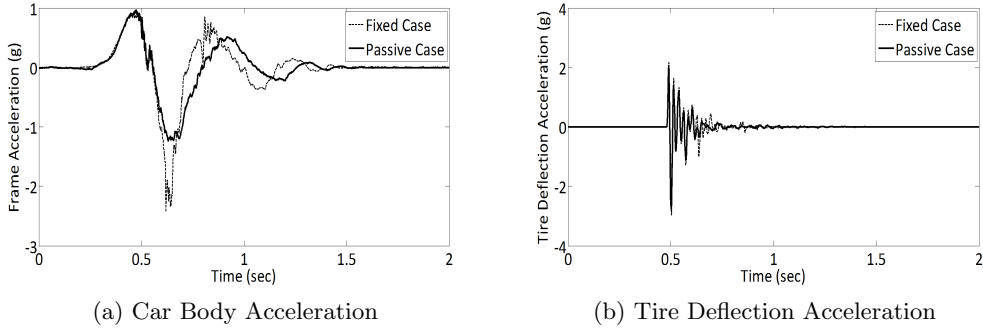


Figure 3: Drop Test Results

Table 1: RMS/APPROXIMATE GAIN VALUES OF EXPERIMENTAL RESULTS
CBA: Car Body Acceleration. TDA: Tire Deflection Acceleration

		Fixed	Passive
Drop (RMS)	CBA (g)	0.4543	0.3710
	TDA (g)	0.2746	0.2396
Sinusoidal (Gain)	CBA	0.6220	0.5170
	TDA	1.3316	1.2944

model.

In the time domain simulation, the vehicle traveling at a steady horizontal speed of 40mph was subjected to a road bump of height 8cm . The Car Body Acceleration, Suspension Deflection, and Tire Deflection responses were compared between the constant stiffness and the passive variable stiffness cases. For the constant stiffness case, the control mass was locked at three different locations ($d = 40\text{cm}$, $d = 45.56\text{cm}$ and $d = 50\text{cm}$). The value $d = 45.56\text{cm}$ is the equilibrium position of the control mass. Next, a simulation was performed for the passive case. The results obtained are shown in Figures 7a, 7b and 6c which are the the car body acceleration, suspension deflection, and tire deflection responses, respectively. Figure 6d shows the position history of the control mass for the passive variable stiffness case.

3 Variable Stiffness Suspension System: Active Case

This work considered the active case of the variable stiffness suspension system. The horizontal strut was used to vary the load transfer ratio by actively controlling the location of the point of attachment of the vertical strut to the car body. The control

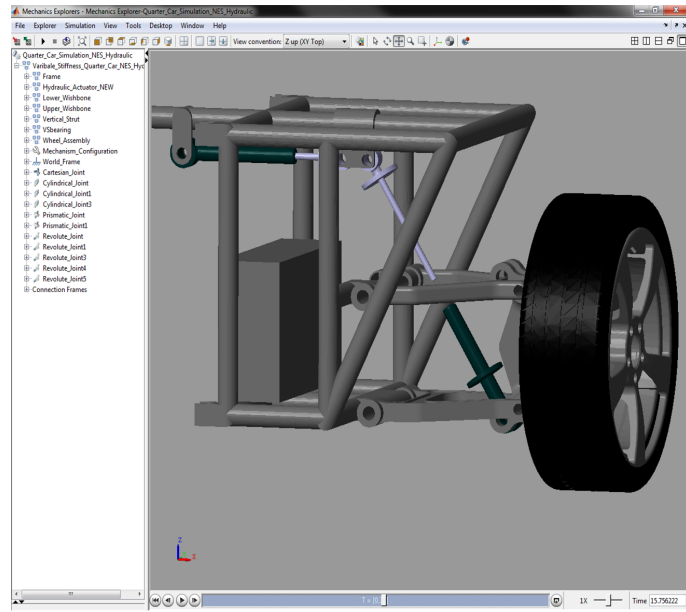


Figure 4: Simmechanic Model

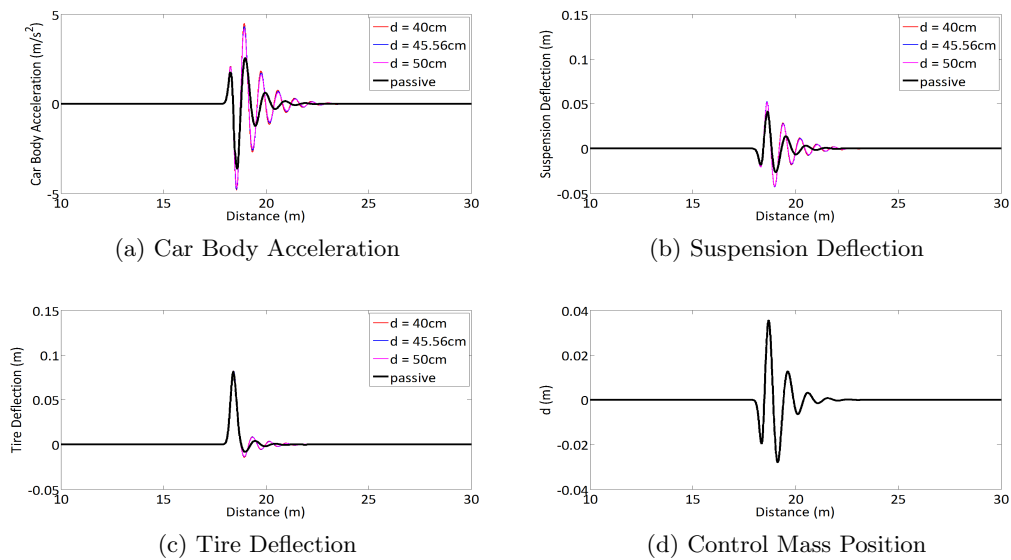


Figure 5: Time Domain Simulation: Passive Case

algorithm, effected by a hydraulic actuator, uses the concept of nonlinear energy sink to effectively transfer the vibrational energy in the sprung mass to a control mass, thereby reducing the transfer of energy from road disturbance to the car body at a relatively

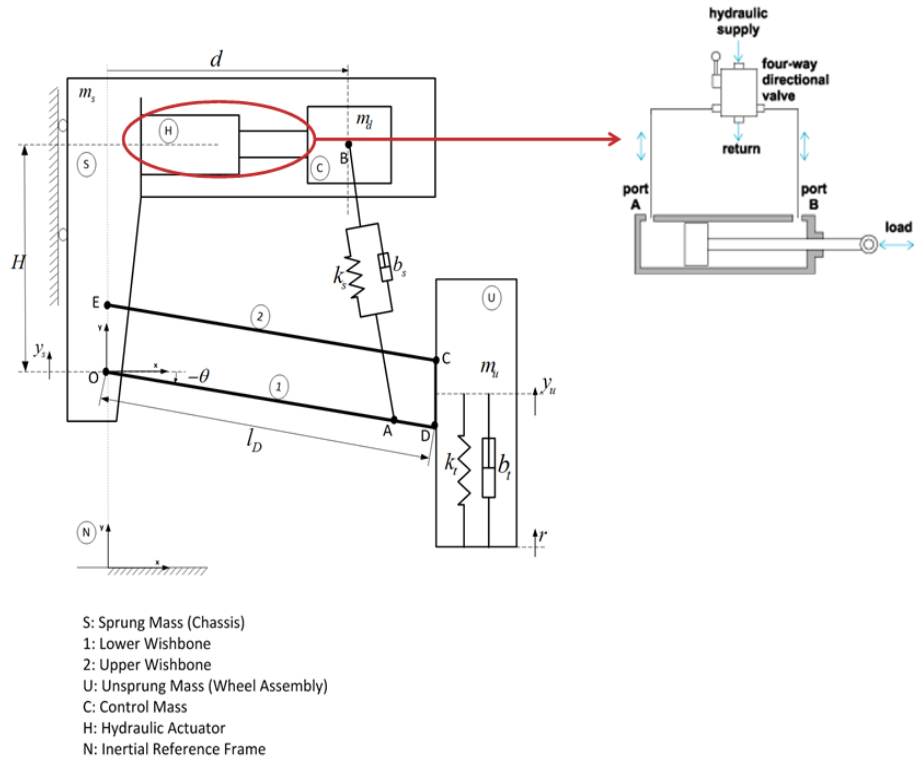


Figure 6: Variable Stiffness Suspension System: Active Case

lower cost compared to the traditional active suspension using the skyhook concept. The analyses and simulation results showed that a better performance can be achieved by subjecting the point of attachment of a suspension system, to the chassis, to the influence of a horizontal nonlinear energy sink system.

Nonlinear Energy Sinks (NES) are essentially nonlinear damped oscillators which are attached to a primary system³ for the sake of vibration absorption and mitigation. Such attachments have been used extensively in engineering applications, particularly in vibration suppression or aeroelastic instability mitigation. The motivation for the use of NES is primarily due to their proven capability to achieve one-way irreversible energy pumping from the linear primary system to the nonlinear attachment. The goal therefore was to achieve a one-way irreversible energy pumping of the road disturbance to the secondary system whose vibration is orthogonal to the car body motion. A fairly general nonlinear function was used in this work, instead of cubic nonlinearity that is generally used.

³This refers to the main system whose vibration is intended to be absorbed

3.1 Control Design

The control development was done using a Lyapunov based adaptive method. First, the error dynamics was reduced using time scale decomposition and Tichonov's Theorem. Next, the update law was designed, and the proof of stability of the error dynamics given using Lyapunov technique. The resulting control and update laws are summarized below:

$$\begin{aligned}
 \text{Desired Force (NES)} \quad F_d &= -k_1(l_{0_d} - d) - k_2 \sinh(\alpha(l_{0_d} - d)) - b_d \dot{d} \\
 \text{Tracking Error} \quad e &= F - F_d \\
 \text{Update Law} \quad \dot{\hat{\Theta}} &= -\Gamma Y e \\
 \text{Fictitious Control} \quad \bar{u} &= Y^T \hat{\Theta} - k_1 e - c_1 \text{sgn}(e) \\
 \text{Slow Control} \quad u_s &= \bar{u} \left(P_s - \text{sgn}(\bar{u}) \frac{F}{A} \right)^{-\frac{1}{2}} \\
 \text{Final Control} \quad u &= -K_f x_v + \frac{1 + K K_f}{K} u_s
 \end{aligned}$$

3.2 Simulation

Similar to passive case, the simulation models were developed using MATLAB Simemechanic, second generation. The following figures show the results obtained for the active case. Also, another very interesting result obtained from this work is that, by designing the active suspension system this way, the power requirement was cut down by 40%. This is because the direction of actuation is nearly orthogonal to the direction of excitation.

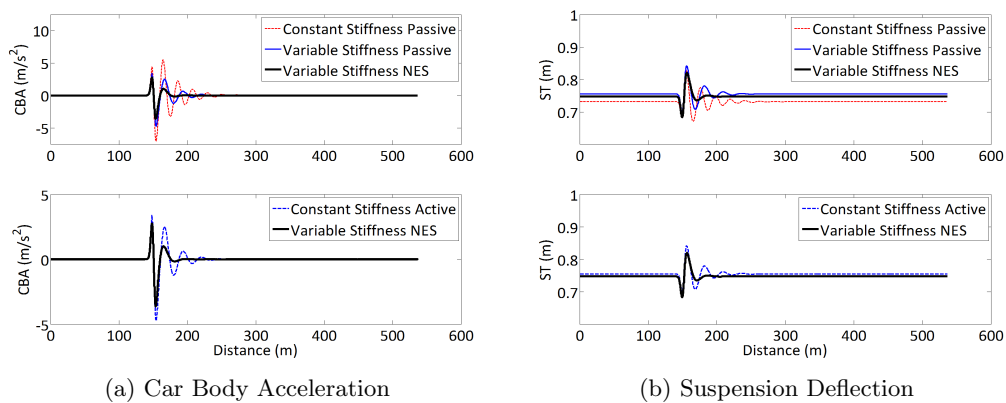


Table 2 shows the variance gain values of the responses for the Constant Stiffness Passive (CSP), Constant Stiffness Active(CSA), Variable Stiffness Passive, and Variable Stiffness NES (NES) cases. For the CSA case, the vertical strut was replaced by a hydraulic actuator, controlled to track the skyhook damping force. The numerical values

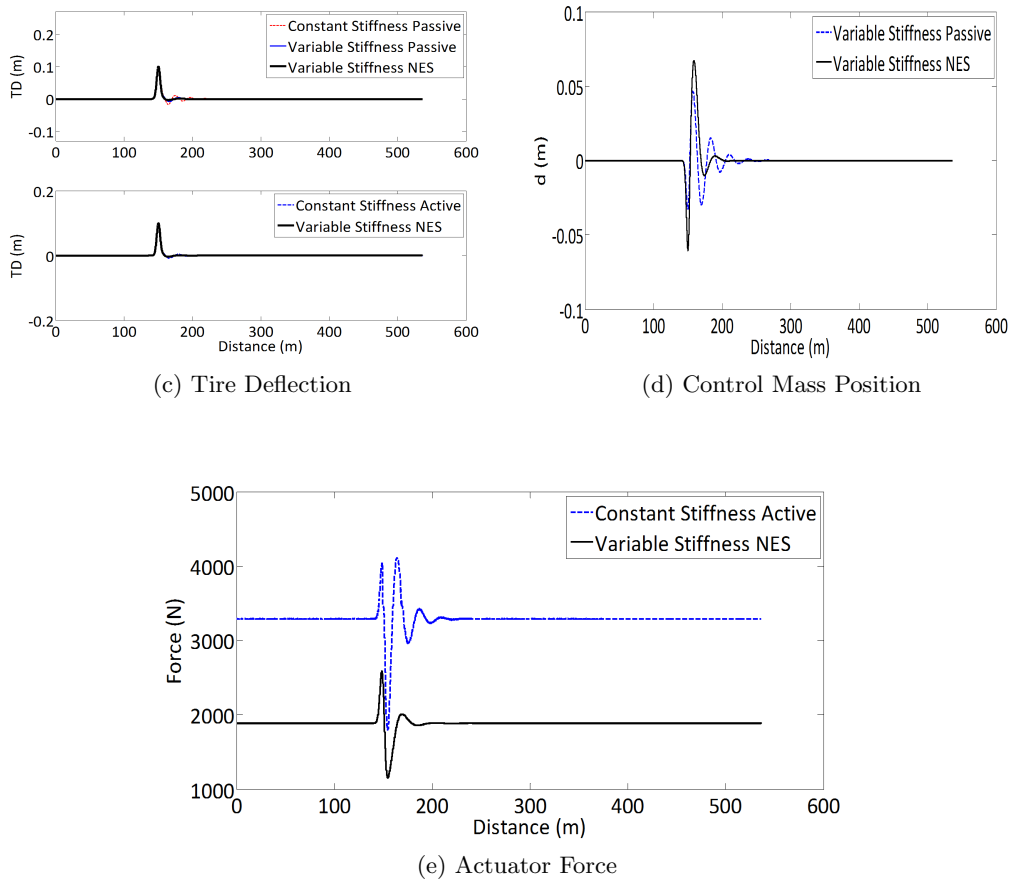


Figure 5: Time Domain Simulation: Active Case

in Table 2 are also displayed graphically in Fig. 6, where the tire deflection values has been scaled by a factor of 50 for better visibility.

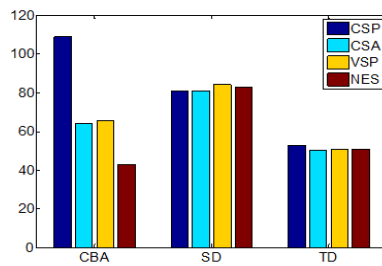


Figure 6: Simulation Results: Active Case

Table 2: VARIANCE GAIN VALUES: ACTIVE

	Constant Stiffness Passive	Constant Stiffness Active	Variable Stiffness Passive	Variable Stiffness NES
Car Body Acceleration (s^{-1})	109.0389	64.2818	65.6127	42.9737
Suspension Deflection	80.8817	80.8725	84.3834	82.6723
Tire Deflection	1.0562	1.0100	1.0188	1.0152

4 Variable Stiffness Suspension System: Semi-active Case

This work considered the semi-active case of the variable stiffness suspension system. It used two MR dampers, one in the vertical direction and the other in the horizontal direction, as shown in Fig. 7. The nonlinear, nonparametric model of the MR damper is also shown schematically in the figure.

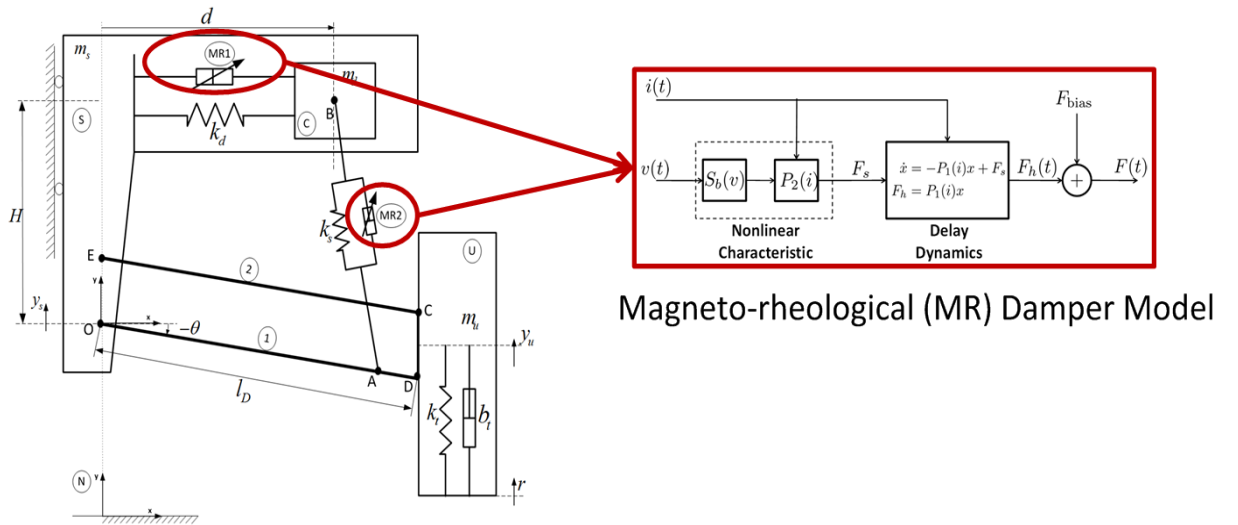


Figure 7: Variable Stiffness Suspension System: Semi-active Case

4.1 Control Design

The control for the vertical MR damper was designed to track the skyhook damping force, while the control for the horizontal MR damper was designed to track the NES. One of the challenges encountered in the control design of the horizontal MR damper is that, while the model of the MR damper is dissipative, the desired NES force is conservative. This means that NES can only be tracked in the passive sub-cycle and not in the active sub-cycle. This problem was resolved by “clipping” the reference NES force in the passivity region of the MR damper. The conservativeness of the NES implies that energy is absorbed from the system and stored during a half-cycle (termed the passive sub-cycle), and supplied back to the system during the next half-cycle (termed the active sub-cycle). Since MR dampers are primarily dissipative, they cannot supply energy to the system. Consequently, “clipping” in the passive region means that the resultant desired force was designed such that energy is dissipated from the system as much as possible, according to the specification of the NES, during the passive sub-cycle, and nothing is done during the active sub-cycle. This was done to ensure a “trackable” desired force for the horizontal MR damper.

The developed control and update laws are summarized in the following algorithm :

Algorithm 4.1: CONTROL/UPDATE($f_d, v, \hat{\Theta}$)

comment: Clipped Desired Force

$$F_d \leftarrow F_d(f_d, v)$$

comment: Compute tracking error

$$e \leftarrow F - F_d$$

comment: Compute control current

$$i_c = \min_{[0 \quad i_{\max}]} \text{roots} \left(-F_d + S_b(v) \hat{P}_2(i) \right)$$

comment: Parameter Update

$$\hat{\Theta} \leftarrow L \int_0^t e(\tau) S_b(v) Y(i_c) d\tau + \hat{\Theta}_0$$

return ($i_c, \hat{\Theta}$)

4.2 Simulation

Similar to the passive and active cases, the simulation models were developed using MATLAB Simmechanic, second generation. The following figures show the results obtained for the semi-active case. Simulations were carried out for the constant stiffness and the variable stiffness suspension systems. For the constant stiffness suspension, the

control mass was locked at a fixed position corresponding to the equilibrium position of the control mass for the variable stiffness system.

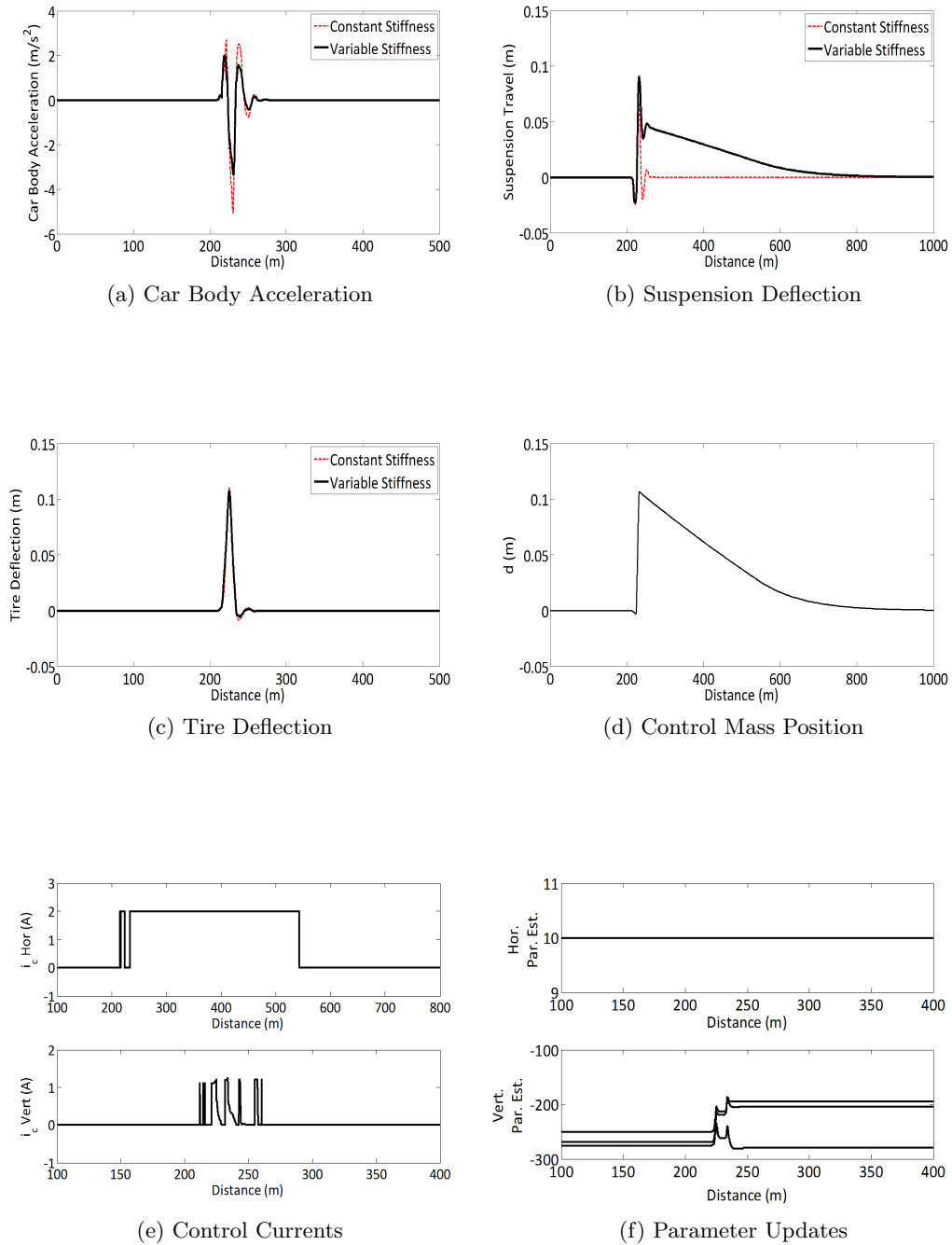


Figure 6: Time Domain Simulation: Semi-active Case

Table 3: VARIANCE GAIN VALUES: SEMI-ACTIVE

	Constant Stiffness	Variable Stiffness
CBA (s^{-1})	50.7306	35.5151
ST	99.9988	112.1389
TD	1.0669	1.0450

Table 3 shows the variance gains for the different responses. Fig 8a shows the car body acceleration, which is used here to describe the ride comfort. The lower the car body acceleration, the better the ride comfort. As seen in the figure, the variable stiffness suspension is a more "ride friendly" suspension, outperforming the traditional vertical skyhook control. As shown in Fig 8b, associated with this improvement is a corresponding degradation in the suspension travel. This agrees with the observation made in earlier sections, as well as the well known trade off between ride comfort and suspension deflection. Fortunately, the 12% degradation in suspension deflection is not as much as the 30% improvement gained in the ride comfort, resulting in an overall better performance. Figure 7d shows the position history of the control mass for the variable stiffness suspension, from which the boundedness of the motion of the control mass is seen. The maximum displacement of the control mass from the equilibrium position is less than 15cm. This implies that the space requirement for the control mass is small, which further demonstrates the practicality of the system. Fig 7c shows that there is no significant reduction in the tire deflection. Thus, the suspension systems are approximately equally "road friendly".

5 Roll Stabilization Using Variable Stiffness Suspension System

Roll dynamics is critical to the stability of road vehicles. A loss of roll stability results in a rollover accident. Typically, vehicle rollovers are very dangerous. Research by the National Highway Traffic Safety Administration (NHTSA) shows that rollover accidents are the second most dangerous form of accidents in the United States, after head-on collision. In 2000, about 9,882 people were killed in the United States in a rollover accident involving light vehicles. Rollover crashes kill more than 10,000 occupants of passenger vehicles each year. As part of its mission to reduce fatalities and injuries, since model year 2001, the National Highway Traffic Safety Administration (NHTSA) has included rollover information as part of its New Car Assessment Program (NCAP) ratings. One of the primary means of assessing rollover risk is the static stability factor (SSF), a measurement of a vehicle's resistance to rollover. The higher the SSF, the lower the rollover risk. Roll stability, on the other hand, refers to the capability of a vehicle to resist overturning moments generated during cornering, that is to avoid rollover. Several factors contribute to roll stability, among which are Static Stability

Factor (SSF), kinematic and compliance properties of the suspension system etc.

In this work, the variable stiffness architecture discussed previously is used in the suspension system to counteract the overturning moment, thereby enhancing the roll stability of the vehicle. The proposed system can be used in conjunction with existing roll stabilization methods, provided that there is no significance interfere with the suspension system.

5.1 Mechanism Description

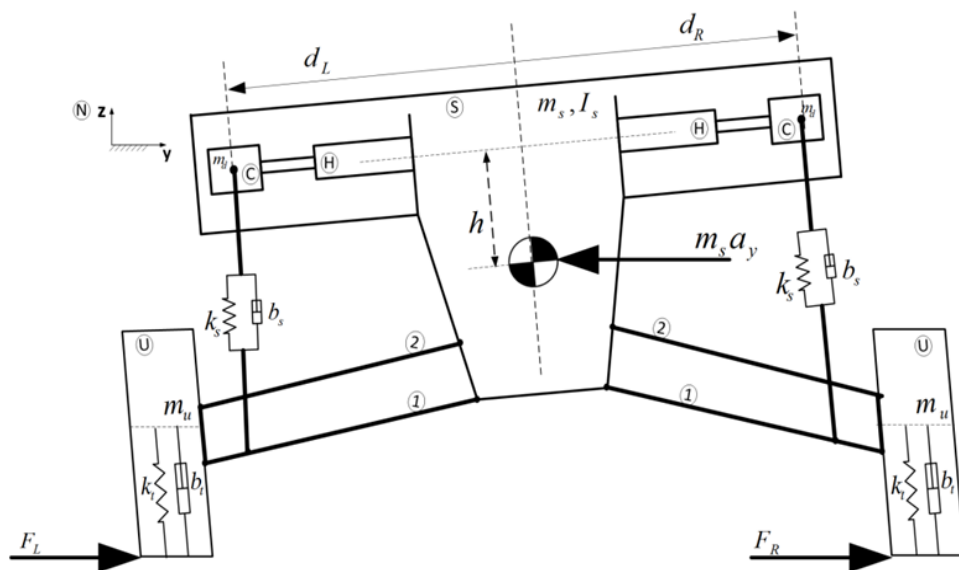


Figure 7: Half Car Model

The schematic diagram of the half car model of the variable stiffness suspension system is shown in Fig 7. The model is composed of a half car body (sprung mass), two identical wheel assemblies (unsprung masses), two vertical spring-damper systems, left and right lower and upper wishbones, hydraulic actuators etc. The main idea of the design is to vary the effective vertical reactive forces of the left and right suspensions to counteract the body roll moments. This is achieved by an appropriately designed control for the hydraulic actuators.

During cornering, a vehicle experiences a radially outwards lateral acceleration acting at the center of mass, as well as corresponding lateral tire forces acting at the tire/road contacts. This results in a roll moment which causes the vehicle to lean outwards. To counteract this roll moment, the outside suspension should become stiffer while the inside suspension should become softer. This generates a counter moment to improve the stability of the roll dynamics.

5.2 Modeling

Fig. 8 shows a schematic of the modeling aspects of the system.

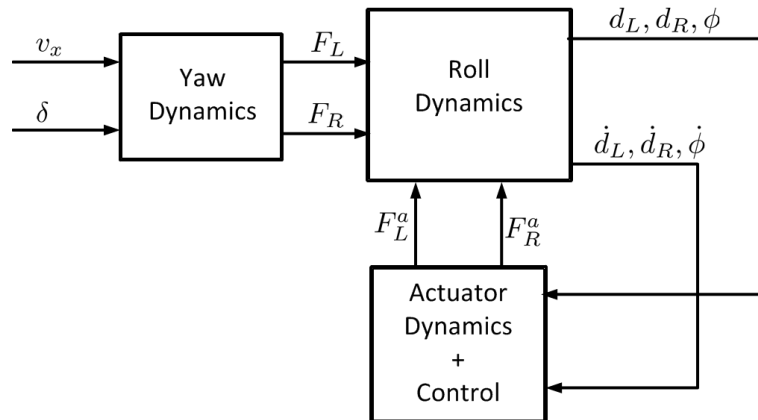


Figure 8: Modeling Schematics

The yaw dynamics of the vehicle was effectively decoupled from the roll dynamics by modeling it as a rigid bicycle in a planar motion. The model has three degrees of freedom. As a result, the yaw dynamics were given by a set of three coupled first order ordinary differential equations. To capture the effect of the nonlinear tire forces at large slip angles, the well known Pacejka “Magic Formula” was used to model the tire lateral forces. The corresponding longitudinal tire forces were obtained by enforcing the friction cone constraint. This was done in order to keep the total tire forces from exceeding the maximum frictional force. The effect of longitudinal load transfer was captured by summing forces in the vertical direction, and taking moments about the body lateral axis, while neglecting pitch dynamics. The roll dynamics was obtained using the free body diagram of an idealized half car model of the system as shown in Fig. 9, where the suspension forces have been replaced with their horizontal components, M_L, M_R , and vertical components N_L, N_R . The assumptions adopted for the roll dynamic model are summarized as follows:

1. The half car body is symmetric about the mid-plane, and as a result the center of mass is located on the mid-plane at a height h above the base of the chassis.
2. The road is level and the points of contact of the tires are on the same horizontal plane.
3. The springs and damper forces are in the linear regions of their operating ranges.
4. The compliance effects in the joints are negligible.

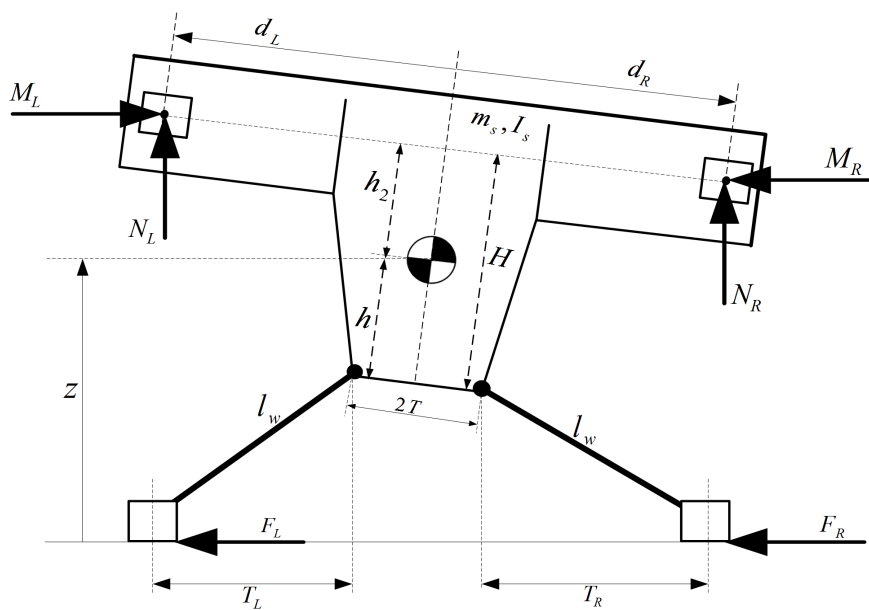


Figure 9: Idealized Half Car Model For Roll Dynamics Modeling

5.3 Parameter Estimation

In order to validate the obtained model, as well as ensure realistic simulations subsequently, the parameters of the roll dynamics are estimated so that the resultant roll dynamics matches the data obtained experimentally. The vehicle used for the data collection is a Toyota Highlander Hybrid 2007 equipped with Inertial Measurement Unit, shown in Fig. 10 during one of the maneuvers. Two sets of data were collected. The first is termed the Circle Data, in which the car is driven around cones arranged on in a circular fashion. The second is termed the Eight Data. Here, the vehicle is driven several times along an eight-shaped path. The data collected for each experiment includes the longitudinal and lateral velocities, lateral acceleration, roll angle and roll rate. The parameters of the model are estimated using the trust-region-reflective method in MATLAB. Figs. 11a and 11c show validations of the estimated parameters against a new Circle Dataset which was not used for the estimation process. Figs. 11b and 11d show similar plots for the Eight Dataset.

5.4 Control Design

The control development was done hierarchically. First for the vehicle body roll, then for the control masses, and finally for the hydraulic actuators. The desired actuator forces required to achieved a desired roll behavior were designed using a model reference adaptive control and sliding mode techniques, then the necessary servo current commands to the spool valve were designed from the actuator dynamics using an adaptive singular

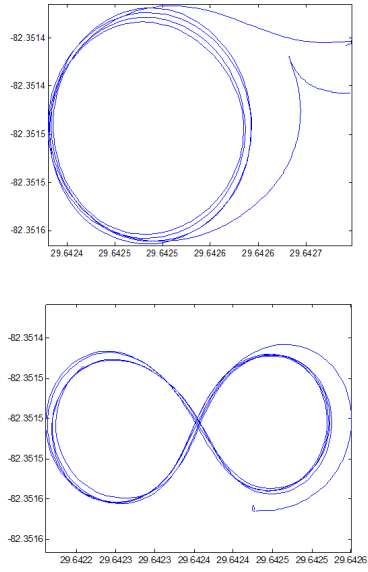
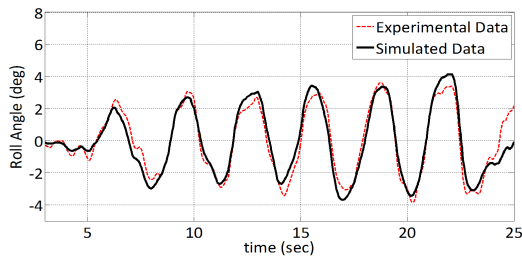
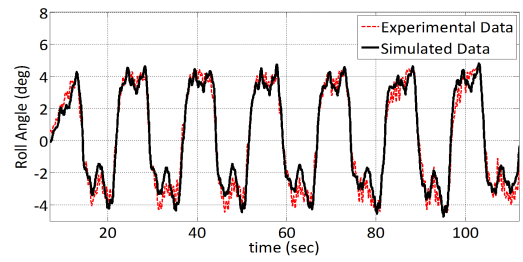


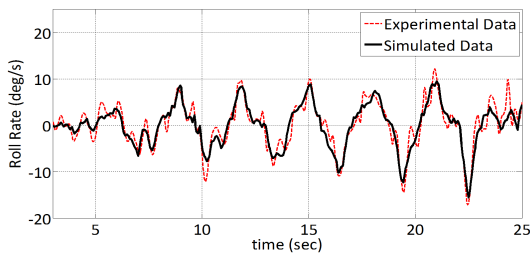
Figure 10: Data Collection Experiment



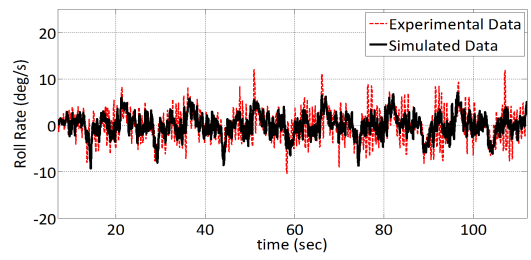
(a) Roll Angle: Circle



(b) Roll Angle: Eight



(c) Roll Rate: Circle



(d) Roll Rate: Eight

Figure 11: Parameter Estimation Validation

perturbation approach. Next, a Lyapunov-based stability analysis was carried out for the overall closed loop error dynamics to guarantee the convergence of the tracking error and boundedness of the system states.

5.5 Simulation

The performance of the proposed control was examined via simulation, using the NTSHA fish hook and the ISO 3888 double lane change maneuvers. The results, shown in the figures below, show that by using the actuated variable stiffness mechanism together with the developed control, the roll angle and roll rates are reduced by more than 50%.

5.5.1 Fish hook Maneuver

The Fish hook maneuver, by NHTSA, is a very useful test maneuver in the context of rollover, in that it attempts to maximize the roll angle under transient conditions. The procedure is outlined as follows, with an entrance speed of 50 mph ($22.352m/s$):

1. The steering angle is increased at a rate of 720 deg/s up to $6.5\delta_{stat}$, where δ_{stat} is the steering angle which is necessary to achieve 0.3g stationary lateral acceleration at 50mph
2. This value is held for 250ms
3. The steering wheel is turned in the opposite direction at a rate of 720deg/s up to $-6.5\delta_{stat}$

The steering angle to the wheels, and the resultant trajectory of the vehicle, for the fish hook maneuver is shown in Fig. 12a.

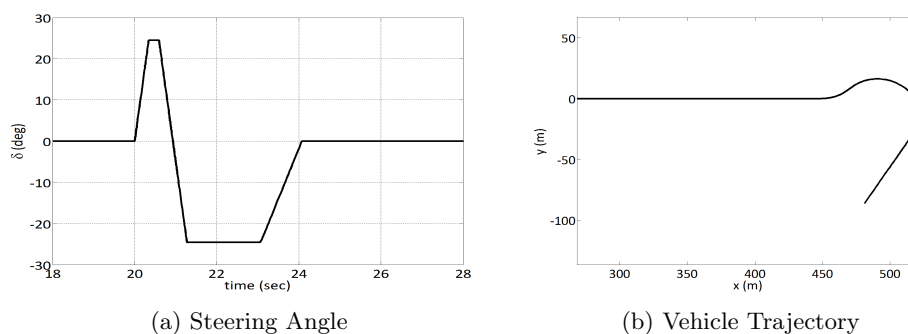


Figure 12: NTSHA Fishhook Maneuver

Figs. 13a and 13b shows the resulting control masses and roll responses respectively, where the constant and variable stiffness cases are plotted together for comparison. These results show that by using the variable stiffness mechanism together with the developed

control algorithm, the roll angle and roll rates are reduced by more than 50%. It is also seen that the control allocation exhibit some ganging phenomenon.

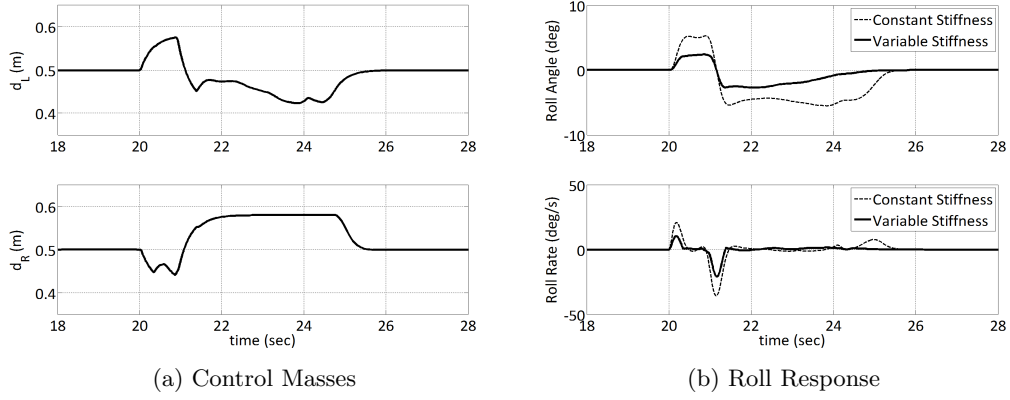


Figure 13: Fishhook Responses

5.5.2 Double Lane Change Maneuver

The ISO 3888 Part 2 Double Lane Change course was developed to observe the way vehicles respond to hand wheel inputs drivers might use in an emergency situation. The course requires the driver to make a sudden obstacle avoidance steer to the left(or right lane), briefly establish position in the new lane, and then rapidly return to the original lane. The steering command to the wheels, and the resultant trajectory of the vehicle, is shown in Figs. 14a and 14b. The corresponding control masses and roll responses are shown in Figs. 15a and 15b, from which it is also seen that the variable stiffness systems shows much better behavior during the severe obstacle avoidance maneuver.

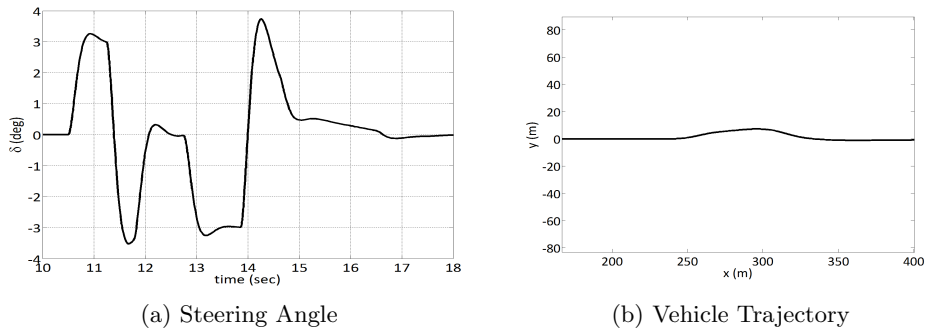


Figure 14: ISO 3888, Part 2, Double Lane Change Maneuver

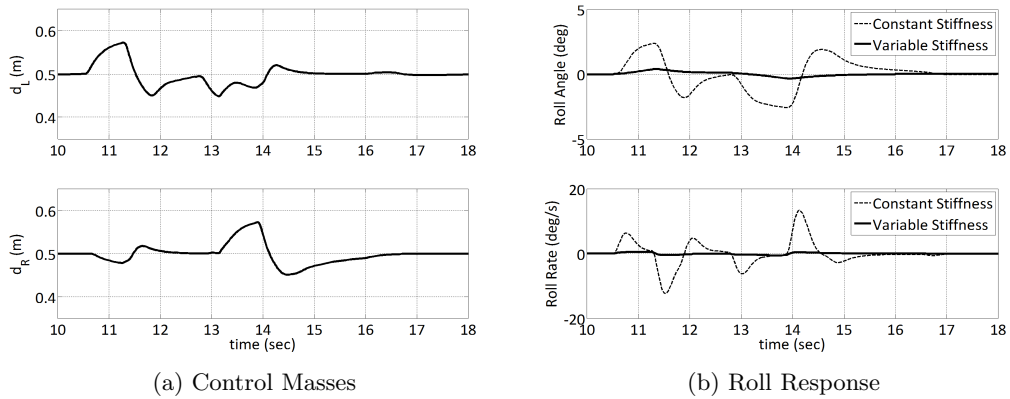


Figure 15: Double Lane Change Response

6 Biography Sketch

Olugbenga Moses Anubi received his B.S (Hons) in systems engineering from the University of Lagos, Nigeria in 2006. He then served in the Nigerian National Youth Service Corp (NYSC) in 2007. He is currently completing his doctoral degree in Mechanical Engineering at the Center for Intelligent Machines and Robotics (CIMAR), at the University of Florida, Gainesville. His research interests are; Vehicle System Dynamics and Control, Suspension Design and Analysis, Nonlinear Control, Robust Control, Optimal Control, Robotics. He is a member of the American Society of Mechanical Engineers (ASME), and the Society of Automotive Engineers (SAE).

